Available online at www.sciencedirect.com
SCIENCE DIRECT®
Journal of Sound and Vibration 283 (2005) 69–90
JOURNAL OF SOUND AND VIBRATION
www.elsevier.com/locate/jsvi

Global control of a vibrating plate using a feedback-controlled inertial actuator

L. Benassi*, S.J. Elliott

Institute of Sound and Vibration Research, University of Southampton, Southampton SO17 1BJ, UK

Received 13 November 2003; accepted 22 March 2004
Available online 12 October 2004

Abstract

Strategies for the suppression of plate vibration are investigated by considering approximations to the equivalent impedance of power-minimizing vibration controllers. The total power transmitted to a plate by both a primary and a secondary point force is minimized and the equivalent impedance presented by the secondary source to the plate is considered.

A novel device for active vibration control, based on an inertial actuator with displacement sensor and local PID controller and an outer velocity feedback control loop, is used to control the vibrating flexible plate. The impedance presented to the plate by this actuator is compared with the equivalent impedance of the optimal active control system. A frequency-domain formulation is used to analyse the stability and performance of an active vibration suppression system using this modified inertial actuator.

The results of an experimental study of active vibration suppression on a flexible plate using the modified inertial actuator are then described. Theory and experiments agree well, demonstrating the effectiveness of the modified inertial actuator.

1. Introduction

Vibration control of flexible structures is an important issue in many engineering applications, especially for the precise operation performances in aerospace systems, satellites, flexible

*Corresponding author. Tel.: +44-23-8059-2689; fax: +44-23-8059-3190.
E-mail address: lb@isvr.soton.ac.uk (L. Benassi).

0022-460X/$ - see front matter © 2004 Elsevier Ltd. All rights reserved.
doi:10.1016/j.jsv.2004.03.039

manipulators, etc. Balancing the stringent performance objectives of modern structures such as superior strength and minimal weight introduces a dynamic component that needs to be considered. Depending on the application, low structural damping can lead to problems such as measurement inaccuracy of attached equipment, transmission of acoustic noise or structural failure. Two types of control methods are generally used to solve this problem: passive control and active control. Passive vibration control and the use of tuned systems can be effective on single-frequency vibrations [1]. This work considers the possibility of broadband control of a distributed system, such as a flexible panel, using local vibration controllers.

A description has been given in Bardou et al. [2] of the performance of two possible strategies that can be used to design an active vibration controller: total power minimization and maximization of the power absorption of the secondary source. Maximization of the power absorption of the secondary source generally reduces the total input power from both primary and secondary sources on an infinite plate. On finite plates, maximizing the power absorption of the secondary sources can result in increases in the total power supplied to the plate, particularly at low frequencies. On the other hand, in the case of finite plates, reductions in total power input can be obtained with a single secondary force or moment adjusted to maximise total input power, but only at the natural frequencies of modes with which these sources can efficiently couple. As long as it is possible to have knowledge of all the power transmission paths, the total power minimization strategy thus offers better results than maximizing the power absorption of the secondary source. Although the strategy of maximizing the power absorbed by the secondary sources should be avoided on structures with strong reflections, it may be worthwhile on more anechoic structures and may be simpler to implement than total power minimization.

In this paper, the total power generated by the forces exerting on the structure is used as a function to be minimized [2]. This approach has also been used in active sound control [3,4]. If we assume the system to be linear such that the velocity fields produced by the forces can be superimposed, then the total power has a known minimum value that is associated with an optimal solution [3,5]. The ratio of the optimal secondary force and the resultant velocity at the secondary force location is termed the equivalent impedance of the active control system. Unfortunately, a drawback of the optimal equivalent impedance is that it is non-causal [6] and so cannot be implemented for broadband random excitations.

A lot of work has been carried out in order to synthesize load impedances which achieve desired performances [7,8], and in this study optimal impedances and sub-optimal impedances generated by passive and active devices will be compared. The goal is to use these devices in order to achieve global control, acting on a local basis. In particular, the use of inertial actuators in active vibration suppression systems is investigated. Inertial actuators do not need to react off a base structure, so that they can be used as modules that can be directly installed on a vibrating structure. It has previously been shown, however, that in order to implement stable skyhook damping with an inertial actuator, the natural frequency of the actuator must be below the first resonance frequency of the structure under control and the actuator resonance should be well damped [9,10].

A vibrating flexible finite plate will be considered in Section 2 and its equivalent impedance for optimal global control will be described. In Section 3, the use of sub-optimal impedances will be considered, generated by a modified inertial actuator with local displacement feedback control. In Section 4, the vibration suppression of a flexible plate is investigated experimentally, using the

modified inertial actuator. In Section 5, the effect of installing the modified inertial actuator at different locations on the flexible plate is analysed. Finally, in Section 6, some overall conclusions are drawn.

2. Optimized impedance for global control of vibrating finite plates

In order to apply the optimal solution to a finite plate, we now examine a single-point secondary force, f_s, acting at a point $P_1 = (x_1, y_1)$, separated by a distance r from a point primary force, f_p, acting at a point $P_0 = (x_0, y_0)$, both forces being applied along the z-axis on a finite plate. This configuration is depicted in Fig. 1. In the simulations, it is assumed that the $700 \times 500 \times 1.85\,\mathrm{mm}^3$ plate is clamped on two opposite ends and free to move on the other two. These particular dimensions and boundary conditions were chosen to correspond to those of the experimental plate described in Section 4 and also used in previous investigations [11]. Y_{00} is the driving point mobility at P_0, defined as $Y_{00} = \dot{z}_0(\omega)/f_0(\omega)$, where $\dot{z}_0(\omega)$ is the velocity in the z-direction evaluated at P_0, and $f_0(\omega)$ is the excitation force at P_0. Y_{10} is the transfer mobility when the point of excitation is P_0 and the measurement occurs at P_1, and Y_{11} is the driving point mobility at P_1. The driving point and transfer mobilities for this system, relating the vertical velocity and the force excitation at the locations P_0 and P_1, can be derived using a modal superposition approach [12–15]. In this study, the system is divided into individual components and the dynamics of each component, modelled either as a lumped or distributed system, is evaluated in terms of input and transfer mobilities or impedances.

It is possible to define a cost function that will be used as the reference for all the remaining computations. The chosen cost function is the total power supplied to the plate, which is given by the sum of the power Π_p due to the primary force acting in P_0 and the power Π_s due to the secondary force acting in P_1. It can be expressed as

$$\Pi = \Pi_p + \Pi_s \tag{1}$$

and rewritten considering that the total power is also one half of the real part of the forces times the complex transverse velocity of the plate at the position of the application of the forces. This

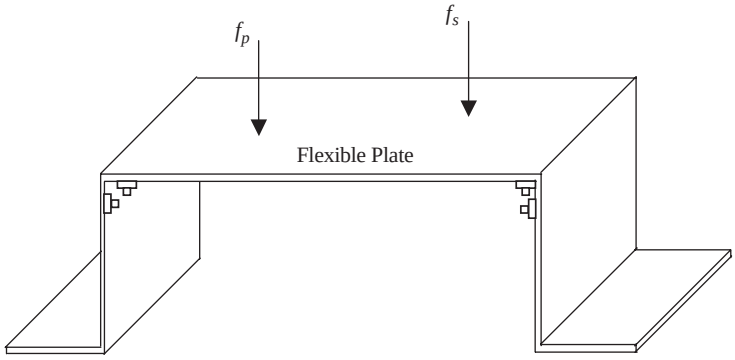

Fig. 1. A point primary force and a point secondary force applied to a finite $700 \times 500 \times 1.85\,\mathrm{mm}^3$ plate clamped on two opposite edges and free on the other two edges.

total power can also be written as [16]

$$\Pi = \tfrac{1}{2}\mathrm{Re}\{f_p^* v_p + f_s^* v_s\} = A|f_s|^2 + f_s^* b + b^* f_s + c, \tag{2}$$

which is a quadratic form where the parameters of the last term of Eq. (2) are

$$A = \tfrac{1}{2}\mathrm{Re}(Y_{11}), \quad b = \tfrac{1}{2}\mathrm{Re}(Y_{10}) f_p, \quad c = \tfrac{1}{2}|f_p|^2 \mathrm{Re}(Y_{00}). \tag{3–5}$$

In particular, the power of the primary force only, which provides the power of the system without any sort of treatment, is given by setting the secondary force in Eq. (2) to zero. This leads to

$$\Pi_p = c. \tag{6}$$

Eq. (2) has a well-defined minimum value [16]

$$\Pi_{\mathrm{opt}} = c - \frac{|b|^2}{A}, \tag{7}$$

which is associated with an optimal secondary force f_{so} given by

$$f_{\mathrm{so}} = -\frac{b}{A} = -\frac{\mathrm{Re}(Y_{10})}{\mathrm{Re}(Y_{11})} f_p. \tag{8}$$

The solid line in Fig. 2 shows the power supplied to the finite plate due to the primary force only, applied at an arbitrary location $P_0 = (0.32\,\mathrm{m}, 0.27\,\mathrm{m})$, and the faint line shows the total power due to the combination of the primary and optimal secondary force, applied at a distance $r = 2\,\mathrm{cm}$, at a location $P_1 = (0.3059\,\mathrm{m}, 0.2841\,\mathrm{m})$, from the primary location. The reduction is

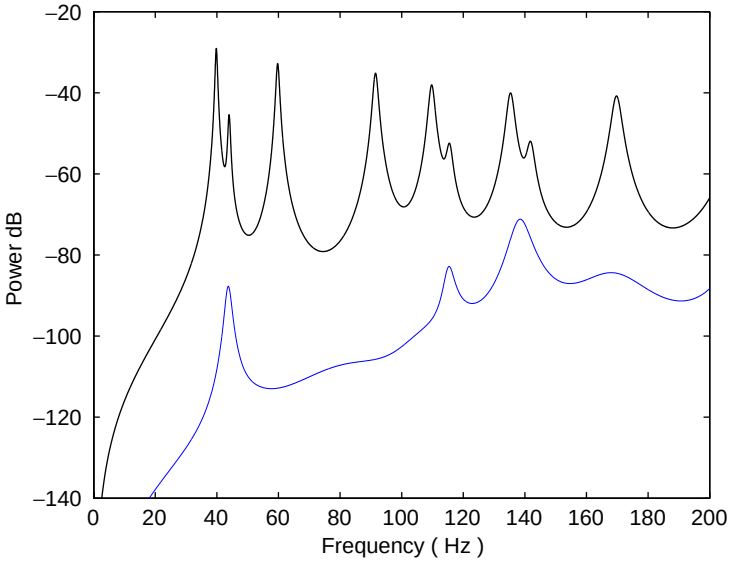

Fig. 2. Total power transmitted to the finite plate due to the primary force only (solid) and due to the primary and secondary forces when the optimal feedforward solution is applied and the distance between primary and secondary force is 2 cm (faint).

substantial, with some of the modes being almost cancelled, while others are greatly reduced. This is due to the particular location that was chosen for the secondary force. At that location, the secondary force can couple into most modes, but this location is either on or close to the nodal lines of those modes that are not completely flattened out. The impedance that the secondary force has to present to the system in order to minimize the total power is obtained by computing the optimal secondary force, f_{so}, per unit velocity at the secondary location, v_{bo}. The velocity of the base v_{bo} at P_1 when the optimal solution is implemented

$$v_{bo} = Y_{10} f_p + Y_{11} f_{so}. \tag{9}$$

Substituting Eq. (8) into Eq. (9), the equation becomes

$$v_{bo} = Y_{10} f_p - Y_{11} \left(\frac{\mathrm{Re}(Y_{10})}{\mathrm{Re}(Y_{11})} \right) f_p, \tag{10}$$

which represents the velocity as a function of the primary force. Combining Eqs. (8) and (10), the impedance when the optimal secondary force is implemented can be obtained. It is given by

$$Z_{opt} = \frac{f_{so}}{v_{bo}} = \frac{\mathrm{Re}(Y_{10})}{\mathrm{Re}(Y_{10}) Y_{11} - \mathrm{Re}(Y_{11}) Y_{10}}. \tag{11}$$

This equivalent impedance, which is entirely reactive [17], is shown in Fig. 3, where sharp transactions between the stiffness-dominated regions and the mass-dominated regions occur. Between 0 and about 45 Hz, below the first natural frequency, the impedance is stiffness

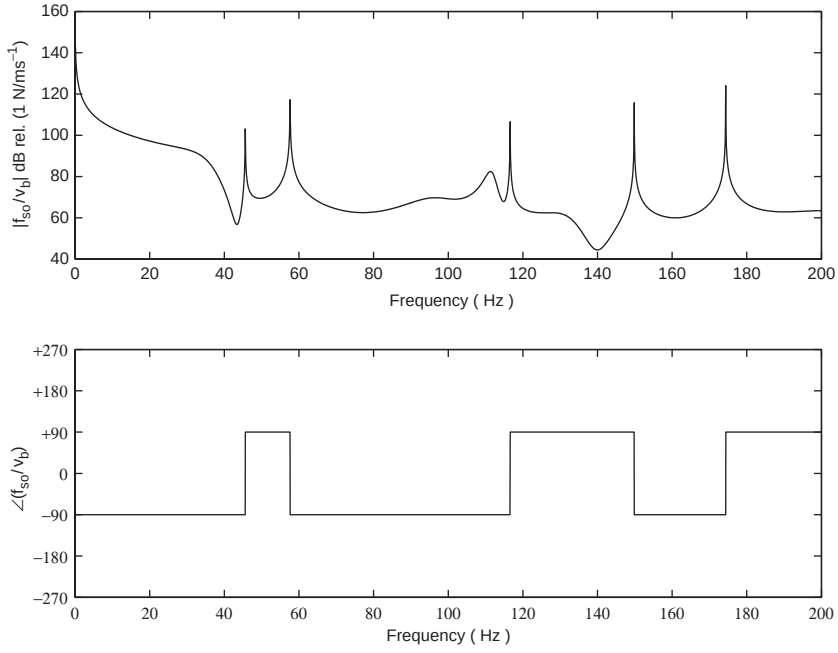

Fig. 3. Equivalent impedance due to the optimal secondary force. The distance between primary and secondary force is 2 cm and the plate is finite. It can be noted that the real part of the impedance is zero.

dominated, as it is between about 60 and 120 Hz, and between 155 and 175 Hz. In the remaining intervals within the 0–200 Hz window, the impedance is mass dominated.

The primary drawback of the optimal equivalent impedance shown in Fig. 3 is that it is non-causal [6] and so cannot be implemented for broadband random excitations. Therefore, other solutions must be investigated even though their performance will be worse than the one provided by the optimal solution. An equivalent impedance of the optimal power minimizing controller on a finite plate, based on the parallel of a spring and a damper, has been investigated by Benassi and Elliott [17]. Attenuation is primarily achieved at low frequencies by the stiffness, and above the first plate resonance by the damper. Adding a stiffness can be seen, in control terms, as skyhook displacement control, while the effect of the dashpot can be interpreted as skyhook damping. Unfortunately, the use of a spring or a damper that react off a rigid base is not often possible in practice. In many practical applications, a rigid ground is not available and the desired impedance must be generated by an inertial (or proof-mass) device.

3. Sub-optimal impedance for global control of vibrating finite plates

The objective of this section is to compare the previous results with solutions obtained using passive and active vibration controllers employing an inertial actuator.

3.1. Mass–spring–damper system on the flexible plate

Fig. 4 shows the case where a passive system, comprising a mass, spring and a damper, is installed on the plate at $P_1 = (0.3059\,\text{m}, 0.2841\,\text{m})$, 2 cm from the primary force at $P_0 = (0.32\,\text{m}, 0.27\,\text{m})$. The values that were used in the simulations for this passive system were chosen to match those in the experimental investigation and were $m_a = 0.24\,\text{kg}$, $c_a = 18\,\text{Ns/m}$ and $k_a = 2000\,\text{N/m}$, where m_a is the moving mass, c_a is the damping of the passive system and k_a is its stiffness. Adding a passive mass–spring–damper system on a finite plate does not imply any

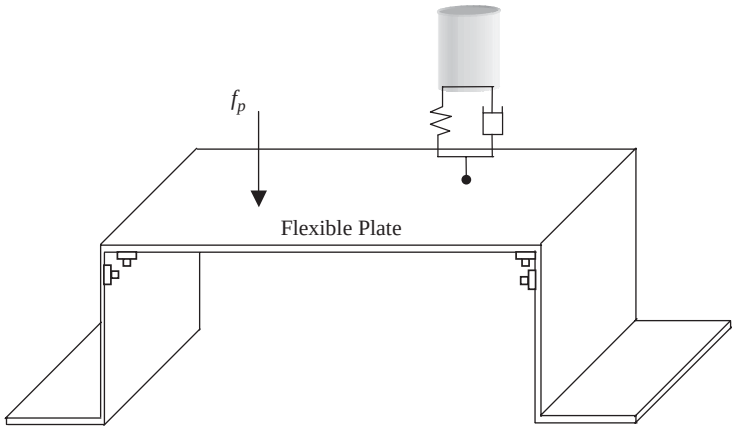

Fig. 4. A point primary force and a point secondary force, obtained through a mass–spring–damper system, applied to a finite $700 \times 500 \times 1.85\,\text{mm}^3$ plate. The plate is clamped on two opposite edges and free on the other two edges.

restriction on the stability margin of the whole structure. Thus, other values of the parameters can be chosen, which will affect performance according to the well-known behaviour of a vibration neutraliser. However, in order to implement skyhook damping with a good stability margin using an inertial actuator, the natural frequency of the actuator must be below the first resonance frequency of the structure under control and the actuator resonance should be well damped [9]. This implies some limitations in the choice of the parameters, as it will be explained in the next section.

The transmitted force, f_t, exerted by a mass–spring–damper system is equal to the secondary force f_s and is given by [10]

$$f_s = f_t = -\frac{j\omega m_a k_a - \omega^2 m_a c_a}{k_a + j\omega c_a - \omega^2 m_a} v_b = -Z_{\text{open}} v_b. \tag{12}$$

The velocity, v_b, of the base at P_1 is given by

$$v_b = Y_{10} f_p + Y_{11} f_t = Y_{10} f_p - Y_{11} Z_{\text{open}} v_b, \tag{13}$$

which can be rewritten as

$$v_b = \frac{Y_{10}}{1 + Y_{11} Z_{\text{open}}} f_p. \tag{14}$$

The total power Π, described by Eq. (2), can be computed from Eqs. (12) and (13). Fig. 5 shows the power of the finite plate and in particular the dashed line shows the effect of the passive

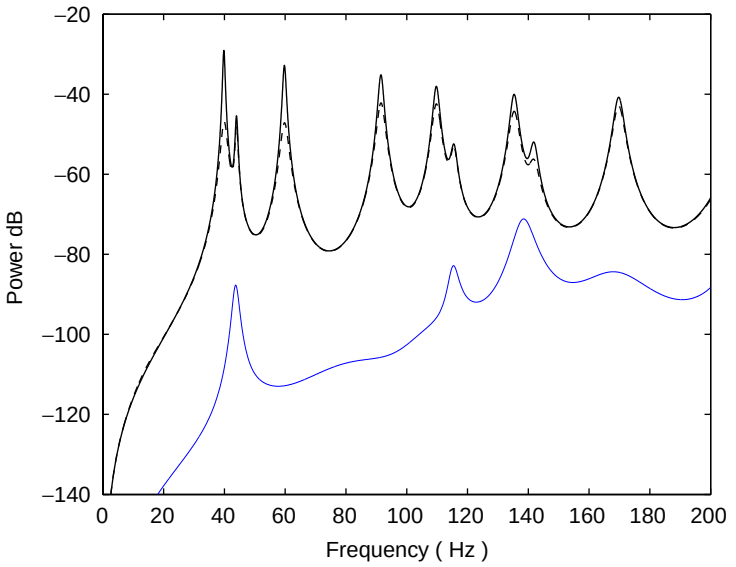

Fig. 5. Total power transmitted to the finite plate due to the primary force only (solid), the primary and secondary forces with the optimal feedforward solution (faint), and the primary and secondary forces when the mass–spring–dashpot system with no other inner loop is applied (dashed). The distance between primary and secondary force is 2 cm.

controller. The addition of the resonance frequency, ω_a, which is given by

$$\omega_a = \sqrt{\frac{k_a}{m_a}} \tag{15}$$

at about 14.5 Hz can be hardly noticed, nor can the fact that the first resonances are slightly shifted to higher frequencies due to the presence of the vibration neutralizer [18]. Although some reduction in the total power is obtained, compared to the case where only the primary force is present, the difference with the optimal solution is large. The impedance of the passive system is shown in Fig. 6. The impedance is passive and it is mass dominated between 0 Hz and the resonance frequency of the passive device, whereas it is mainly damping dominated at higher frequencies. The behaviour of the magnitude of the impedance is typical of the dynamic response of a vibration neutralizer, which is quite different from the optimal solution in Fig. 3. This difference in the impedance presented to the system explains the considerable difference in performance, together with the fact that the damping value of the actuator is 18 Ns/m, which is much less than that calculated in Section 2 that is required for optimal control (4000 Ns/m).

3.2. Inertial actuator with local displacement feedback and plate velocity feedback on the flexible plate

An inertial actuator has a mass, a ''proof-mass'', supported on a spring and driven by an external force. The force in small actuators is normally generated by an electromagnetic circuit.

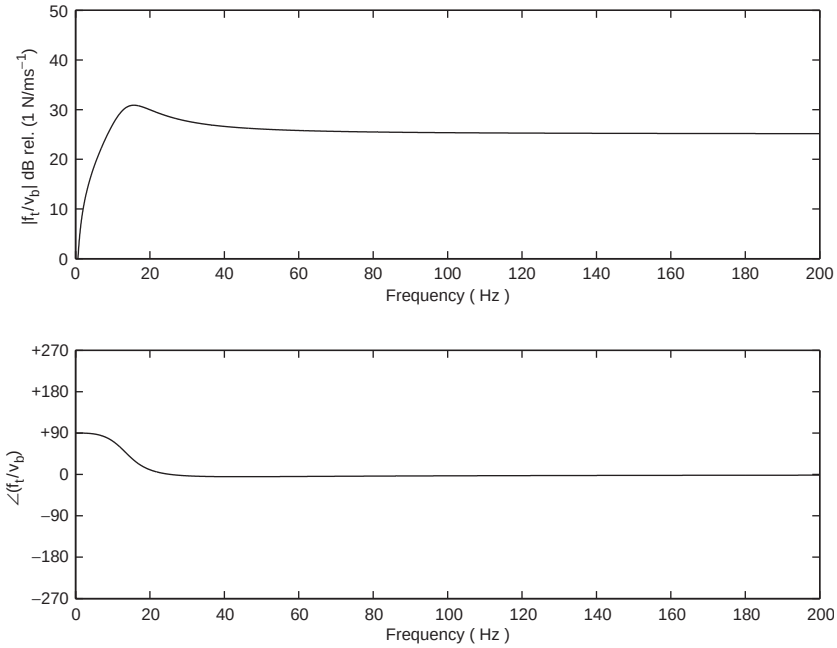

Fig. 6. Mechanical impedance of the mass–spring–dashpot system.

The suspended mass can either be the magnets with supporting structure or in some cases the coil structure. The transduction mechanism which would supply the force to the system is not modelled in detail because its internal dynamics are typically well beyond the bandwidth of the structural response. Fig. 7 illustrates the case where a modified inertial actuator, based on an inertial actuator with local displacement feedback, described in Ref. [19], is installed on the plate. The measured displacement of the proof mass relative to the inertial actuator's base is fed to a PID controller, which modifies the frequency response of the actuator. If it is necessary to reduce the resonance frequency of the actuator because it is greater than or equal to the first structural mode of the system that needs to be isolated, this can be done with a negative position feedback gain. If this action induces unwanted deflections because of the low stiffness of the closed-loop system, then a self-levelling mechanism can be employed, which is based on a integral displacement feedback. By doing so, however, the overall system gets closer to instability and additional damping is needed. Another reason why damping may be necessary is if an outer velocity feedback is to be implemented. It was shown by Elliott et al. [9] that this kind of system is conditionally stable and the vicinity to the $(-1,0)$ point in the Nyquist plot depends on how well damped the inertial actuator is. For these reasons, the implementation of a local rate feedback control turns out to be very effective in increasing the damping of the actuator. A modified actuator resonance frequency at about 8 Hz was considered sufficient in this case since the first plate resonance is at about 35 Hz. The values within the PID controller that were used in the simulations are: proportional gain $g_P = -1000$, integral gain $gI = 10{,}000$, and differential gain $g_V = 18$. The secondary force f_s is equal to the transmitted force f_t exerted by the device and its

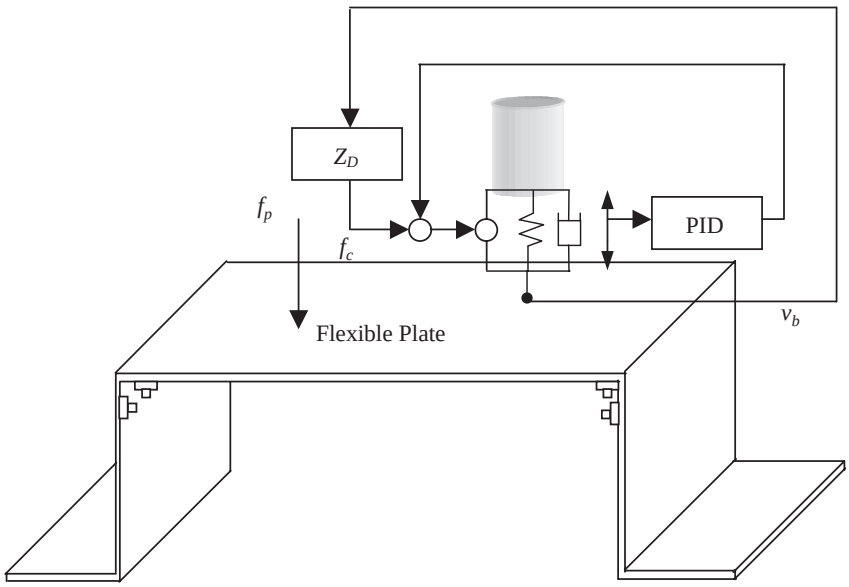

Fig. 7. A point primary force and a point secondary force, obtained through the modified inertial actuator with outer velocity feedback control, applied to a $700 \times 500 \times 1.85\,\text{mm}^3$ plate obtained through the modified inertial actuator. The plate is clamped on two opposite edges and free on the other two edges.

equation, as a function of the command signal, f_c, and the plate velocity at P_1, v_b, is given by [19]

$$f_s = f_t = \frac{-\omega^2 m_a}{-\omega^2 m_a + \mathrm{j}\omega c_a + k_a + g_P + g_I/(\mathrm{j}\omega) + \mathrm{j}\omega g_V} f_c - \frac{(\mathrm{j}\omega m_a k_a - \omega^2 m_a c_a) \cdot (g_P + g_I/(\mathrm{j}\omega) + \mathrm{j}\omega(g_V + Z_a))}{(-\omega^2 m_a + \mathrm{j}\omega c_a + k_a + g_P + g_I/(\mathrm{j}\omega) + \mathrm{j}\omega g_V)\mathrm{j}\omega Z_a} v_b, \tag{16}$$

where $Z_a = c_a + k_a/(\mathrm{j}\omega)$. The command force, f_c, will be used to implement the outer velocity feedback control loop. Eq. (16) can be grouped as

$$f_t = T'_a f_c - Z'_a v_b, \tag{17}$$

where T'_a and Z'_a are the blocked response and mechanical impedance of the actuator [19], as modified by the local displacement feedback. The base velocity at P_1 is given by

$$v_b = Y_{10} f_p + Y_{11} f_t, \tag{18}$$

Substituting Eq. (17) into Eq. (18) the base velocity is computed as a function of the primary force f_p and the control command f_c:

$$v_b = \frac{Y_{10}}{1 + Y_{11} Z'_a} f_p + \frac{Y_{11} T'_a}{1 + Y_{11} Z'_a} f_c. \tag{19}$$

When the outer velocity feedback loop, described by

$$f_c = -Z_D v_b, \tag{20}$$

is implemented, the choice of the outer gain Z_D becomes important in order to guarantee a good performance. Fig. 8 shows the ratio of the frequency-averaged power between power of the controller (without outer loop) and the active control (with outer loop) as a function of the outer velocity feedback gain, Z_D, assuming that the feedback loop is stable. The minimum of the function at $Z_D = 2080$ indicates the value of the gain that provides the greatest attenuation in terms of power. In this case, the attenuation is about 11.2 dB. In terms of stability, when the device is installed and the outer velocity feedback control loop is implemented based on the measurement of v_b, the Nyquist plot of the second term of Eq. (19) provides the means to determine the stability of the closed-loop system [20]. The theoretical active controller becomes unstable when the outer velocity feedback gain is greater than 2410, as can be deduced from the Nyquist plot in Fig. 9. In the simulations, a velocity feedback gain of $Z_D = 150$ was chosen in order to guarantee a 6 dB stability margin when the additional phase shifts present in the experimental system are accounted for [21]. This implies, from Fig. 8, that an attenuation of only about 4 dB can be achieved. When the outer velocity feedback loop in Eq. (20) is implemented, the base velocity, described in Eq. (19), becomes

$$v_b = \frac{Y_{10}}{1 + Y_{11} Z'_a + Y_{11} Y'_a Z_D} f_p. \tag{21}$$

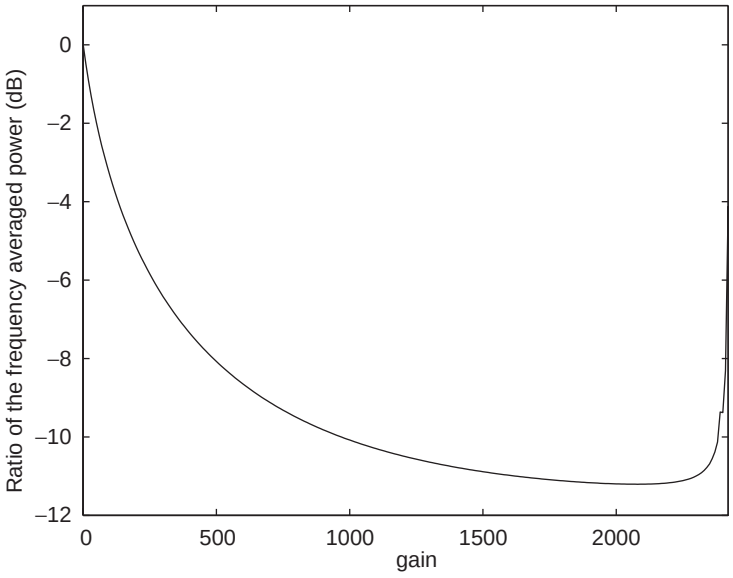

Fig. 8. Ratio of the frequency averaged total power transmitted to the plate with the modified actuator before and after the outer feedback loop is implemented, as a function of the outer velocity feedback gain Z_D. The minimum of the function at $Z_D = 2080$ indicates the value of the gain that provides the greatest attenuation (about 11.2 dB) in terms of power. The active controller becomes unstable for outer velocity gains $Z_D > 2410$. The distance between primary and secondary forces is 2 cm.

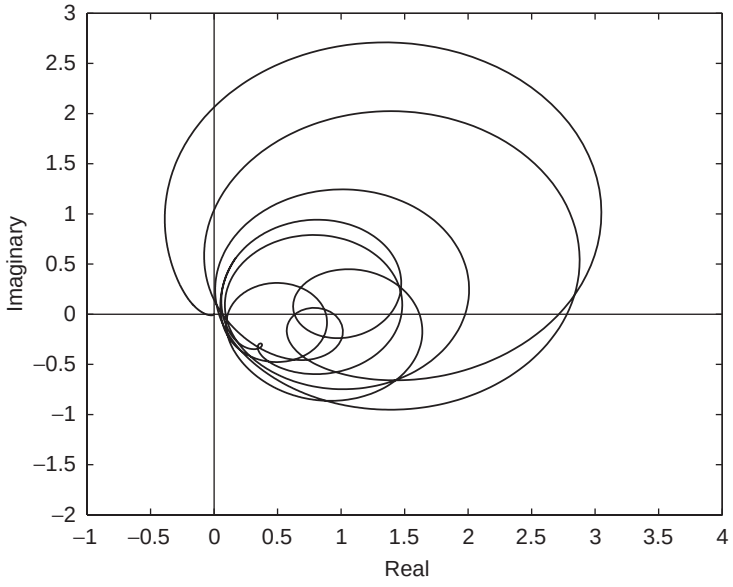

Fig. 9. Nyquist plot of the idealised open loop system when the modified inertial actuator is applied and an outer velocity feedback control loop is implemented. The distance between primary and secondary force is 2 cm and the plate is finite. The values within the PID controller that were used in the simulations are: $g_P = -1{,}000$, $g_I = 10{,}000$, $g_V = 18$, and the outer velocity feedback gain $Z_D = 150$.

Substituting Eq. (20) into Eq. (16), the transmitted force, f_t, as a function of the bas velocity, v_b, is given by

$$f_t = -\frac{(\mathrm{j}\omega m_a k_a - \omega^2 m_a c_a)\cdot(g_P + g_I/(\mathrm{j}\omega) + \mathrm{j}\omega(g_V + Z_a)) - \mathrm{j}\omega^3 Z_a Z_D}{(-\omega^2 m_a + \mathrm{j}\omega c_a + k_a + g_P + g_I/(\mathrm{j}\omega) + \mathrm{j}\omega g_V)\mathrm{j}\omega Z_a} v_b. \tag{22}$$

Once the base velocity in Eq. (21) is computed, then the transmitted force in Eq. (22) can be obtained and therefore the total power can be calculated. This is plotted in Fig. 10, where it can be noted that the reduction of the total power due to the modified inertial actuator (dashed line) is greater than the results obtained with the passive treatment, shown in Fig. 5. Although the difference with the optimal solution is still large, useful reductions in power are predicted, which shows that the modified inertial actuator can be used effectively in reducing the vibration of panels. The impedance presented by the active mount to the system is given by Eq. (22), which is plotted in Fig. 11. The impedance is not passive, unlike the previous case, and it is mainly damping dominated at frequencies greater than the inertial actuator's resonance frequency. As explained in Ref. [19], this is due to the choice of the local feedback gains, and in particular the derivative term within the PID controller. At high frequencies, the impedance tends to $Z_D + c_a + g_V$. Thus, out of the three gains within the inner PID controller, the derivative term plays an important role in the performance results when the outer velocity feedback control loop is implemented. Ideally, its value should be chosen such that the modified inertial actuator's input impedance is damping controlled [19]. In conclusion, the modified inertial actuator with outer velocity feedback loop is an effective way of adding damping to the system.

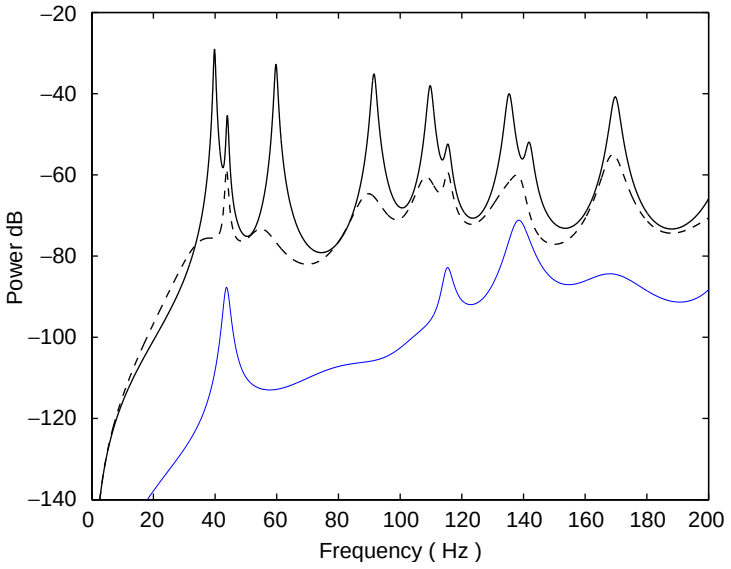

Fig. 10. Total power transmitted to the finite plate due to the primary force only (solid), the primary and secondary forces when the optimal feedforward solution is applied (faint), and when the feedback system, based on the modified inertial actuator and an outer feedback loop with $Z_D = 150$, is applied (dashed). The distance between primary and secondary force is 2 cm.

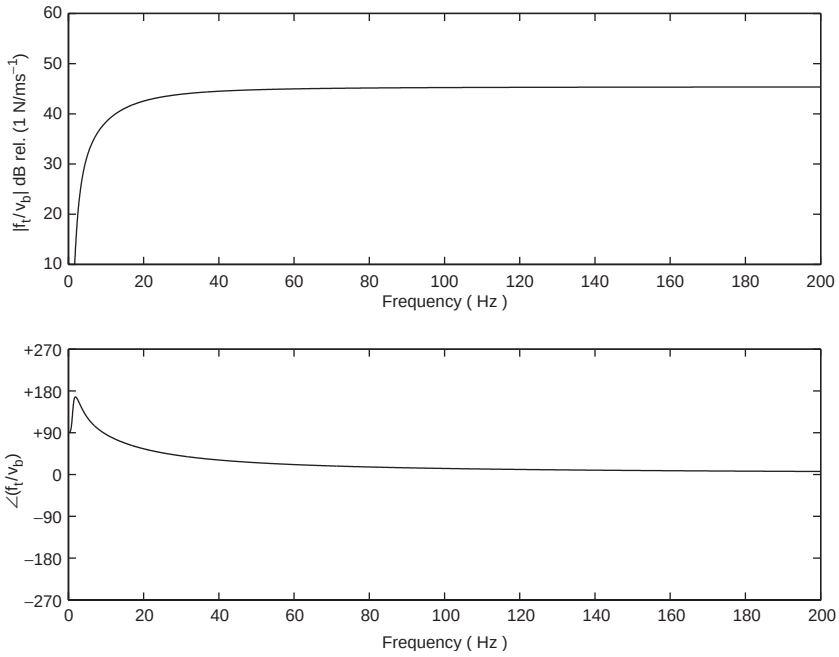

Fig. 11. Mechanical impedance of the inertial actuator with inner and outer feedback loops when the local displacement feedback control and the outer velocity feedback control are implemented. In particular, $g_P = -1000$, $g_I = 10{,}000$, $g_V = 18$ and $Z_D = 150$.

When the outer control gain Z_D is chosen to be the equivalent impedance described in Eq. (11), the control system turns out to be unstable. If the outer feedback controller is an integrator of the form $Z_D{=}k_D/(\mathrm{j}\omega)$, interesting results are obtained. Choosing such a control impedance implies that only the first part of the optimal impedance in Eq. (11) is considered. In other words, k_D is chosen to be the low-frequency passive approximation of the optimal solution. In particular, when $k_D = 550{,}000\,\mathrm{N/m}$ (the same value was chosen as the passive approximation for this system in Ref. [17]), the closed-loop system turns out to be conditionally stable, and a 6 dB stability margin is guaranteed. This is shown in the Nyquist plot in Fig. 12, where the curve at low frequency intersects the real axis at about –0.5. The total power for this case is plotted in Fig. 13, where the reduction of the total power due to the modified inertial actuator and the outer controller, based on the passive approximation of the optimal solution, is quite outstanding and not very dissimilar from the optimal solution. At low frequency, attenuations of more than 40 dB can be obtained, which indicates that the panel vibrations are almost suppressed. Unfortunately in real systems, due to low-frequency phase shifts of the electronic components [21], the stability margin of the system is greatly reduced and the performance of the closed-loop system is not dissimilar to the outer velocity feedback case. By considering an outer feedback controller of the form $Z_D{=}k_D/(\mathrm{j}\omega)$, stiffness is added to the system (also illustrated in the impedance plot in Fig. 14) and this implies that the peaks in Fig. 13 are moved to higher frequencies. This is beneficial in the low-frequency range [17], but those peaks are not suppressed, they are simply moved to higher

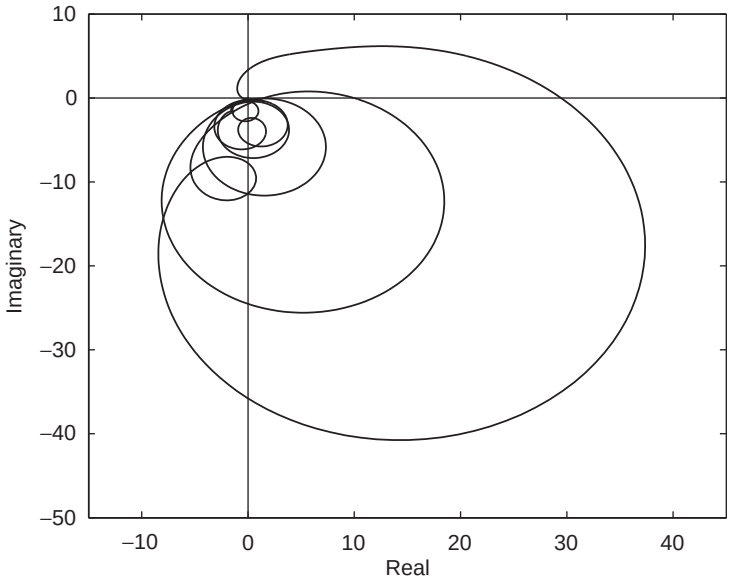

Fig. 12. Predicted Nyquist plot of the open-loop system when the modified inertial actuator is applied and an outer feedback control loop, based on an integrator of the form $Z_D/(j\omega)$, is implemented. The distance between primary and secondary force is 2 cm and the plate is finite. The values within the PID controller that were used in the simulations are: $g_P = -1{,}000$, $g_I = 10{,}000$, $g_V = 18$, and the outer feedback gain $Z_D{=}k_D/(j\omega)$, where $k_D = 550{,}000$.

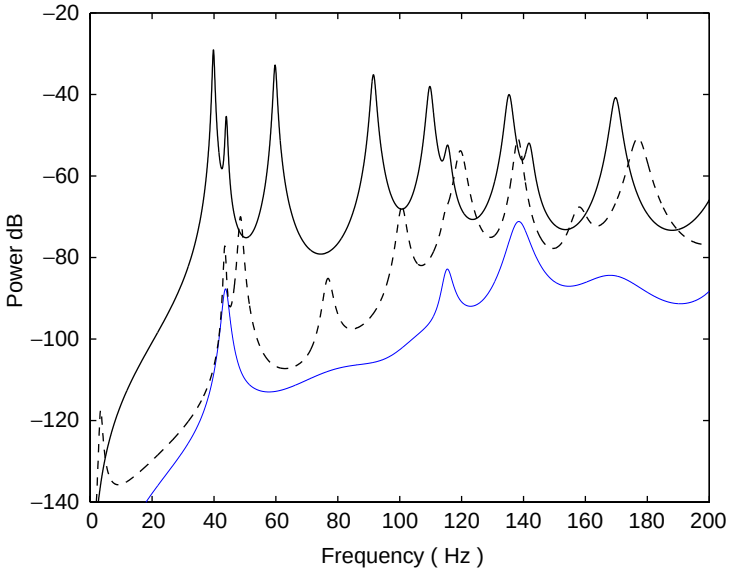

Fig. 13. Total power transmitted to the finite plate due to the primary force only (solid), the primary and secondary forces with the optimal feedforward solution (faint), and the primary and secondary forces when the modified inertial actuator and the outer feedback controller, based on a passive approximation of the optimal solution $Z_D{=}k_D/(j\omega)$ with $k_D = 550{,}000$, are applied (dashed). The distance between primary and secondary force is 2 cm.

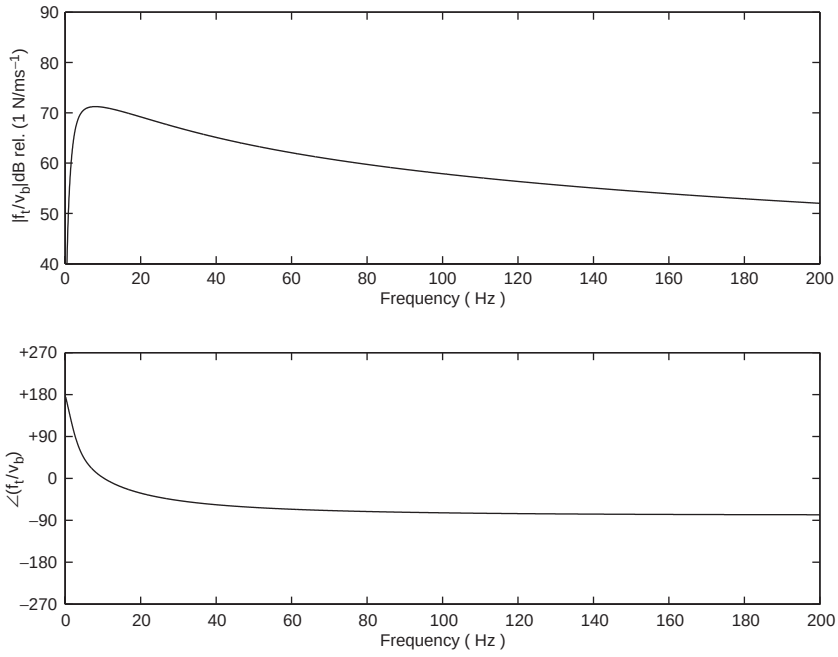

Fig. 14. Mechanical impedance of the inertial actuator with inner and outer feedback loops when the local displacement feedback control and the outer integral feedback control are implemented. In particular, $g_P = -1{,}000$, $g_I = 10{,}000$, $g_V = 18$ and Z_D=$k_D/(\mathrm{j}\omega)$, where $k_D = 550{,}000$.

frequencies. Also, a portion of the inertial actuator resonance which occurs at low frequency is greatly amplified because of the integral velocity feedback control law. The impedance presented to the system is plotted in Fig. 14. It is not passive, and it is mainly stiffness dominated, except at very low frequency, where a phase shift occurs. The magnitude of the impedance is "that of the dynamic response of a vibration neutralizer", which is quite different from the optimal solution in Fig. 3.

4. Experiments on active vibration suppression with the modified inertial actuator

In this section, we consider the practical use of an inertial actuator with local feedback for the active suppression of a vibrating flexible plate. The arrangement is illustrated in Fig. 15. It consists of a flexible steel plate $700 \times 500 \times 1.85\,\mathrm{mm}^3$, clamped on the two longer sides [22], on which is mounted a modified inertial actuator. The primary force is provided by an LDS Ling 401 shaker, placed underneath the plate. The inertial actuator used for the experiments to produce the control force was a mechanically modified version of an Active Tuned Vibration Absorber (ATVA) manufactured by ULTRA Electronics, described in detail in Ref. [23] and shown in Fig. 14, from which the internal springs were removed, leaving the proof mass ($m_a = 0.24\,\mathrm{kg}$) attached to the case by eight thin flexible supports. This modification in the stiffness (so that $k_a = 2000\,\mathrm{N/m}$) changed the actuator resonance frequency from 73.8 to 14.5 Hz [19]. The measured damping ratio

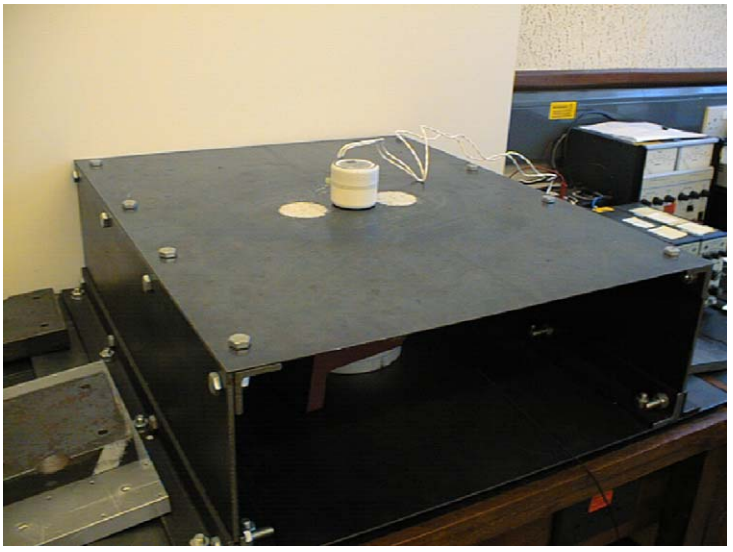

Fig. 15. The experimental arrangement, which consists of a finite flexible plate, driven by a primary force (shaker underneath), and controlled by a modified ULTRA Electronics inertial actuator placed on the flexible plate.

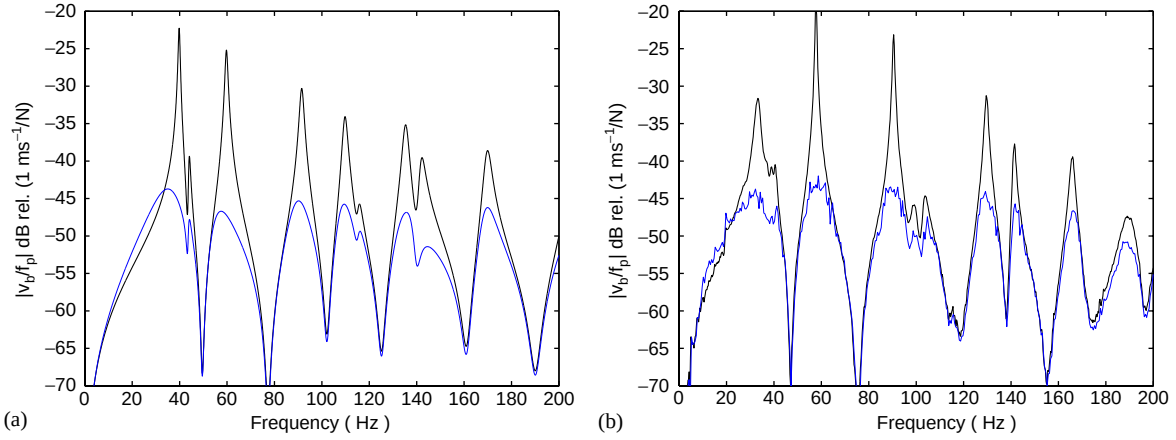

Fig. 16. Predicted (a) and measured (b) frequency response of the plate velocity at the secondary location per primary excitation when no control is implemented (solid), and when both the modified inertial actuator and the outer velocity feedback loop are implemented with $Z_D = 150$ (faint). Under experimental conditions, stability is guaranteed when $Z_D < 300$.

was used to estimate the damping factor as $c_a = 18\,\mathrm{Ns/m}$. An inner displacement feedback loop is used to modify the response of the inertial actuator, as discussed above, and an outer velocity feedback system is used to provide active skyhook damping for the equipment. The values of the gains within the PID controller were chosen in order to provide a modified inertial actuator with the characteristics described in Section 3.2. In this experimental configuration, an outer velocity

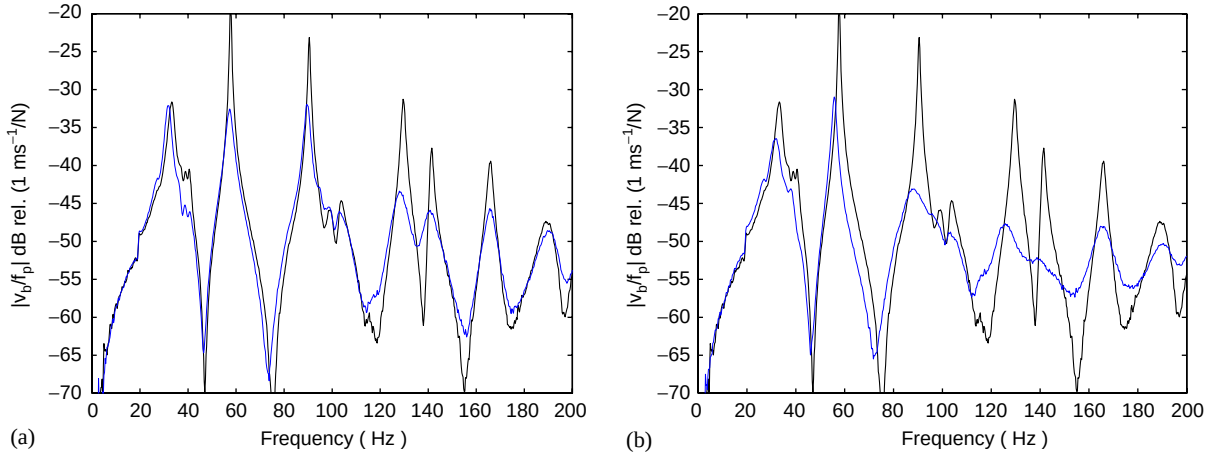

Fig. 17. Measured frequency response of the plate velocity at the secondary location per primary excitation when no control is implemented (solid), when a passive vibration absorber, based on foam, is installed and covers the whole plate (a, faint), and when a passive vibration absorber, based on foam and aluminium layers, is installed and covers the whole plate (b, faint).

feedback control gain $Z_D = 150$ was chosen, which guarantees a 6 dB stability margin. Fig. 16(a) shows theoretical prediction of the equipment velocity per unit primary excitation for the uncontrolled and the control cases when the relative distance is 2 cm. Good vibration isolation conditions can be achieved by the modified inertial actuator and the outer velocity feedback loop. The outer loop, with response Z_D, improves the behaviour of the plate, but it also enhances its frequency response at low frequency, as predicted by the conditional stability of the closed loop system. The corresponding measured data are shown in Fig. 16(b), where a 20 dB reduction at the first plate resonance frequencies was observed. The theoretical prediction and the experimental measurements agree well, demonstrating the effectiveness of the active control system based on a modified inertial actuator with local displacement feedback control.

This result was compared with an entirely passive vibration control method, when the flexible plate was entirely covered by either a passive unconstrained viscoelastic layer, composed of foam, or a 2.5-cm-thick passive constrained layered absorber, composed of the same viscoelastic material with layers of aluminium. Fig. 17 shows the measured data, compared to the uncontrolled case. Although the passive treatment is equally or slightly more effective at higher frequencies, compared with Fig. 16(b), it is much less effective then the active treatment at lower frequencies. The mass of the first passive coating was 0.275 kg, while the mass of the second passive coating was 0.645 kg, which compared to either the mass of the proof mass (0.24 kg) or the mass of the whole modified inertial actuator (0.42 kg) confirms the potentiality of the active solution.

4.1. Kinetic energy analysis of the active vibration suppression system with the modified inertial actuator

The control performance of the active vibration suppression system with the modified inertial actuator has been re-examined based on the kinetic energy. To calculate the true kinetic energy of

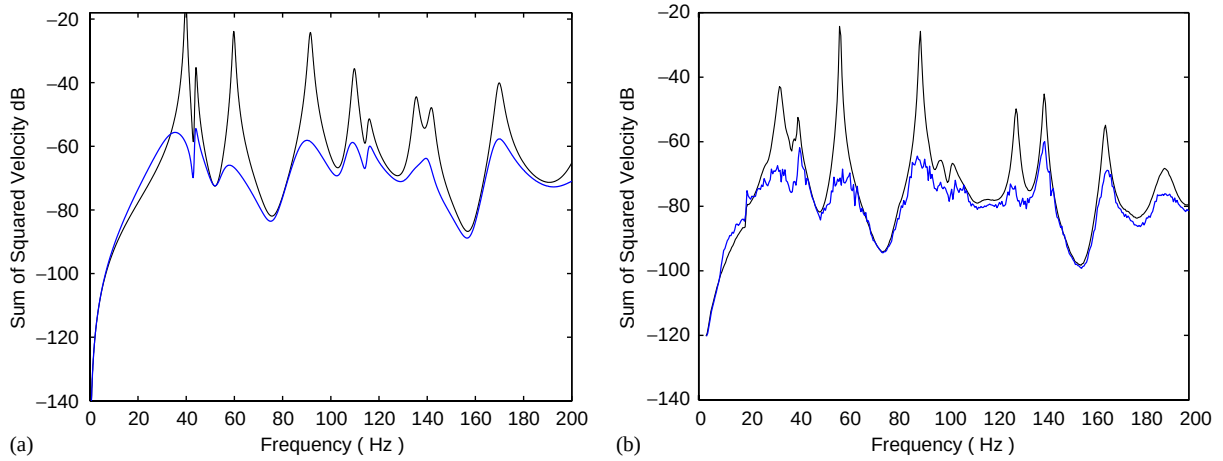

Fig. 18. Predicted (a) and measured (b) sum of square velocities of the plate when no control is implemented (solid), and when both the modified inertial actuator and the outer velocity feedback loop are implemented with $Z_D = 150$ (faint).

the system, the vibration of both the rigid body modes and the flexible body modes would have to be accounted for. In the experiments, however, only the plate velocities at 40 locations were measured, when the modified inertial actuator with outer velocity feedback loop was installed at the same location as described above. The sum of squared velocities at each location is therefore used to evaluate the control performance of the system. Fig. 18 shows the predicted and experimental results, which lead to similar conclusions as those drawn in the previous section. Theory and measurements agree well, showing up to 20 dB reduction in the vibration level and demonstrating the effectiveness of the modified inertial actuator.

5. Variation of performance with the location of the modified inertial actuator

The objective of this section is to compare the previous results with solutions obtained by placing the modified inertial actuator with outer velocity feedback loop in other locations on the flexible plate.

Fig. 19 shows the contour plot of the ratio of the frequency-averaged power between power of the uncontrolled plate and the controlled plate using a modified inertial actuator and no outer loop, as a function of the x and y positions of the actuator on the flexible plate. In other words, the primary force is assumed to be at a location $P_0 = (0.32\,\text{m}, 0.27\,\text{m})$, which guarantees that a sufficient number of modes are excited, while the controller, based on the modified inertial actuator with no outer loop, is assumed to be installed in turn on the plate at different locations. For this purpose, 500 potential secondary locations were selected. Fig. 19 shows that the controller achieves at least a 3 dB reduction in the ratio of the frequency-averaged power not only around the location of the primary force, as expected, but also at symmetrical locations on the plate. This distribution obviously changes if the location of the primary force changes. When the outer velocity feedback loop is implemented, the choice of the outer gain Z_D becomes important

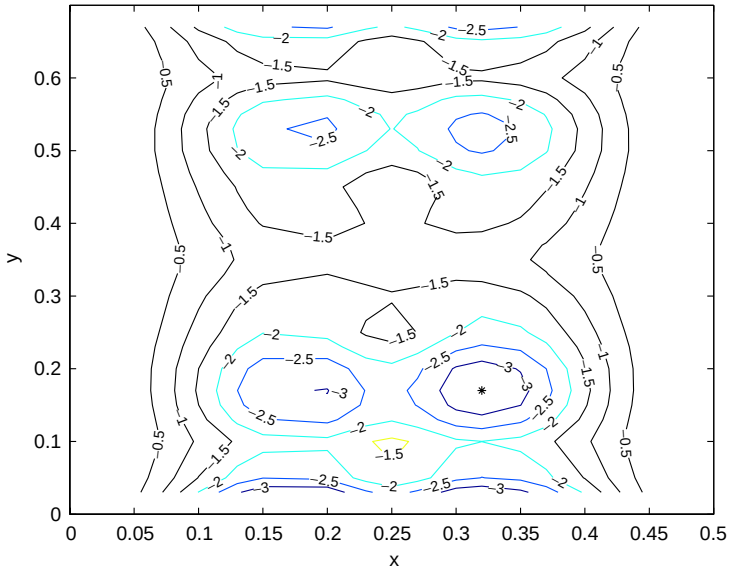

Fig. 19. Contour plot of the ratio of the frequency-averaged power between power of the uncontrolled and the controlled plate with the modified inertial actuator and no outer loop, as a function of the x and y positions of the controller on the flexible plate. The location of the primary force is indicated with a *.

in order to guarantee a certain stability margin and good performance. As Fig. 8 shows, the ratio of the frequency-averaged power between power of the controller (without outer loop) and the active control (with outer loop), as a function of the outer velocity feedback gain is Z_D, has a minimum, which indicates the value of the gain that provides the greatest attenuation in terms of power. When the active control, based on the modified inertial actuator with outer velocity feedback loop, is implemented, the value of the feedback control gain Z_D that minimizes the ratio of the frequency-averaged power can be computed at each of the 500 selected locations on the plate, and is shown in Fig. 20. For each case, the stability of the closed-loop system was guaranteed, although no specific stability margin was set. Depending on the location, the maximum gain Z_D before instability can change considerably, but the gain which minimizes the ratio of the frequency-averaged power was always computed to be less or equal than the stability limit. In Fig. 20 three main regions can be identified: around the location of the primary force high outer loop gains are needed in order to achieve the best attenuation possible with the active controller. High gains are also required close to the clamped edges. In the rest of the plate, although there are some differences, lower gains are needed. Fig. 21 shows the contour plot of the ratio of the frequency-averaged power when the gains in Fig. 20 are used in the outer feedback loop controller. In other words, Fig. 21 shows the best attenuation that can be obtained with the active controller for that specific primary force location. If the active controller is placed near the primary force, average attenuations of up to 12.9 dB can be achieved within the selected frequency range between 0 and 200 Hz, using the high outer gains shown in Fig. 20. This attenuation is decreased down to about 9 dB if the active controller is installed about 8 cm away from the primary force, where the x-direction seems to be a little more privileged than the y-direction in

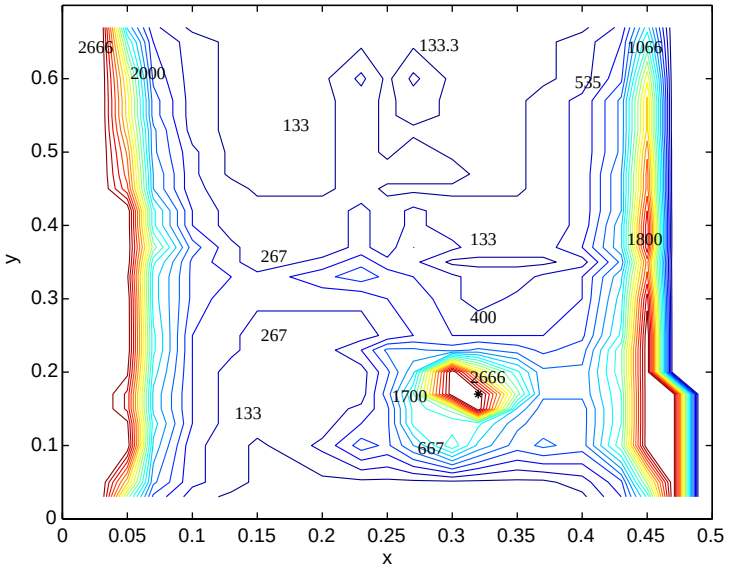

Fig. 20. Contour plot of the outer velocity feedback gain Z_D which, for a specific location, provides the minimum of the ratio of the frequency-averaged power between power of the plate with no actuator and the plate with the modified inertial actuator and outer velocity feedback loop, as a function of the x and y positions of the controller on the flexible plate. The location of the primary force is indicated with a *.

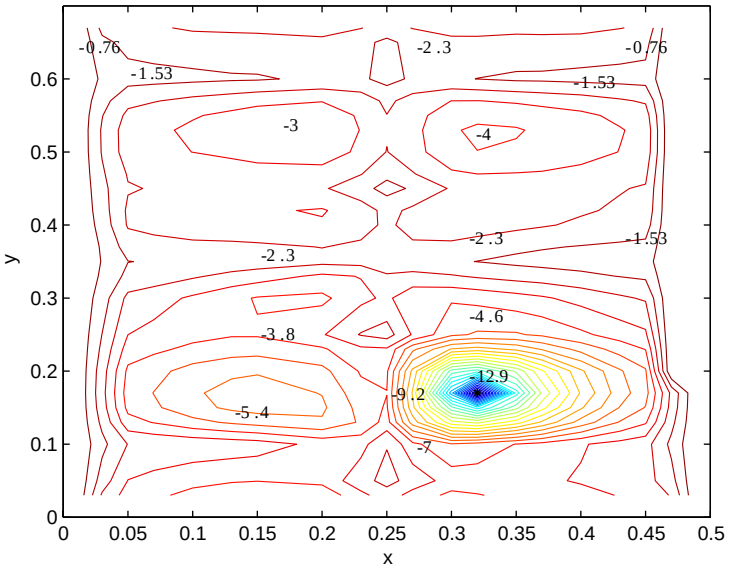

Fig. 21. Contour plot of the ratio of the frequency-averaged power between power of the plate with no actuator and the plate with the modified inertial actuator and outer velocity feedback loop, as a function of the x and y positions of the controller on the flexible plate. The controller is based on the modified inertial actuator with outer velocity feedback loop, whose gain Z_D for a specific location was chosen from the corresponding location in Fig. 20. The location of the primary force is indicated with a *.

terms of attenuation. Although high gains are needed along the edges, as shown in Fig. 21, the attenuation is not significant, while in the rest of the plate attenuations, which vary from 2.3 to 5.4 dB, can be obtained, depending on the location of the secondary force.

In summary, the performance of the control strategy, based on the modified inertial actuator with outer velocity feedback control, depends on both the relative distance between primary and secondary forces as well as their absolute location on the plate. Ideally, the best solution would be to install the controller as close as possible to the primary disturbance.

6. Conclusions

In this study, the total power of the forces exerting on a structure was minimized and a comparison was made between optimal solutions and the performance of various passive and active control treatments involving inertial actuators. In particular, the optimized impedance for global control was compared to the performance of a modified inertial actuator. It was found that, although the optimal impedance is able to provide a more substantial total power reduction than the other treatments, the modified inertial actuator can still guarantee a good power reduction, especially when combined with an outer velocity feedback controller. This seems to be a very promising solution to the vibration suppression problem, even though attention must be paid to the location of the secondary force in order to achieve the best possible attenuation.

In using an inertial actuator for active vibration isolation, the resonance frequency should be lower than the first natural frequency of the system under control and it should be well damped. Actuators with very low resonance frequencies, however, have large static displacements due to gravity. The modified inertial actuator solves this problem. It is based on an inertial actuator and a local PID feedback loop which uses the measurement of the relative displacement between the actuator base and the actuator moving mass. The control law is the sum of an integral term, which provides self-levelling and solves the sagging problem, a derivative term, which provides the device with sufficient initial damping to guarantee a very good stability margin, and a positive or negative proportional term, which determines the actuator resonance frequency. The phase shifts due to transducer-conditioning circuitry limit the maximum gain which can be achieved in the outer loop of the actuator before instability. In the current arrangement, a maximum gain of only 150 N/m s has been used, which only gives an impedance close to the optimal value when the actuator is positioned some distance from the primary source, as shown in Fig. 20. Much larger reductions in power output from a single primary force are, in principle, possible if the destabilizing phase shifts could be reduced and the inertial actuator was placed close to the primary excitation with a gain which was perhaps ten times that currently used.

References

[1] M.J. Brennan, J. Dayou, Global control of vibration using a tunable vibration neutralizer, *Journal of Sound and Vibration* 232 (3) (2000) 585–600.

[2] O. Bardou, P. Gardonio, S.J. Elliott, R.J. Pinnington, Active power minimization and power absorption in a plate with force and moment excitation, *Journal of Sound and Vibration* 208 (1) (1997) 111–151.

[3] S.J. Elliott, P. Joseph, P.A. Nelson, M.E. Johnson, Power output minimizations and power absorption in the active control of sound, *Journal of the Acoustical Society of America* 90 (5) (1991) 2501–2512.
[4] S.J. Sharp, P.A. Nelson, G.H. Koopman, A theoretical investigation of optimal power absorption as a noise control technique, *Journal of Sound and Vibration* 251 (5) (2002) 927–935.
[5] P.A. Nelson, S.J. Elliott, *Active Control of Sound*, Academic Press, New York, 1992.
[6] D.W. Miller, S.R. Hall, A.H. von Flotow, Optimal control of power flow at structural junctions, *Journal of Sound and Vibration* 140 (3) (1990) 475–497.
[7] P.J. Titterton, Synthesis of optimal, single-frequency, passive control laws, with applications to reducing the acoustic radiation from a submerged spherical shell, *Journal of the Acoustical Society of America* 105 (4) (1999) 2261–2268.
[8] D. Guicking, J. Melcher, R. Wimmel, Active impedance control in mechanical structures, *Acoustica* 69 (1989) 39–52.
[9] S.J. Elliott, M. Serrand, P. Gardonio, Feedback stability limits for active isolation systems with reactive and inertial actuators, *Journal of Vibration and Acoustics* 123 (2001) 250–261.
[10] L. Benassi, S.J. Elliott, P. Gardonio, Active vibration isolation using an inertial actuator with local force feedback control, *Journal of Sound and Vibration* 276 (2004) 157–179.
[11] L. Benassi, P. Gardonio, S.J. Elliott, Equipment isolation of a SDOF system with an inertial actuator using feedback control strategies, *Proceedings of the ACTIVE2002 Conference*, Southampton, UK, 15–17 July 2002.
[12] W. Soedel, *Vibration of Shells and Plates*, Marcel-Dekker, New York, 1993.
[13] L. Cremer, M. Heckl, E.E. Ungar, *Structure-borne Sound*, Springer, Berlin, 1988.
[14] R.E.D. Bishop, D.C. Johnson, *The Mechanics of Vibration*, Cambridge University Press, Cambridge, 1960.
[15] A.W. Leissa, *Vibration of Plates*, NASA SP-160, 1969.
[16] C.R. Fuller, S.J. Elliott, P.A. Nelson, *Active Control of Vibration*, Academic Press, New York, 1997.
[17] L. Benassi, S.J. Elliott, The equivalent impedance of power-minimising vibration controllers on plates, *Journal of Sound and Vibration* 283 (1 + 2) (2005) 47–67, this issue; doi:10.1016/j.jsv.2004.03.060.
[18] Den Hartog, *Mechanical Vibrations*, Dover Publications, New York, 1985.
[19] L. Benassi, S.J. Elliott, Active vibration isolation using an inertial actuator with local displacement feedback control, *Journal of Sound and Vibration* 278 (2004) 705–724.
[20] G.F. Franklin, *Feedback Control of Dynamic Systems*, 3rd ed., Addison-Wesley, Reading, MA, 1994.
[21] K.A. Ananthganeshan, M.J. Brennan, S.J. Elliott, High and low frequency instabilities in feedback control of a vibrating single-degree-of-freedom system, *Proceedings of the ACTIVE2002 Conference*, Southampton, UK, 15–17 July 2002.
[22] M. Serrand, Direct Velocity Feedback Control of Equipment Velocity, M.Phil. Thesis, University of Southampton, 2000.
[23] R. Hinchliffe, I. Scott, M. Purver, I. Stothers, Tonal active control in production on a large turbo-prop aircraft, *Proceedings of the ACTIVE2002 Conference*, Southampton, UK, 15–17 July 2002.